



Published in final edited form as:

J Am Chem Soc. 2016 August 24; 138(33): 10561–10570. doi:10.1021/jacs.6b05484.

Synthesis and biological evaluation of kibelone C and simplified derivatives

Janjira Rujirawanich^a, Soyeon Kim^b, Ai-Jun Ma^a, John R. Butler^a, Yizhong Wang^a, Chao Wang^a, Michael Rosen^b, Bruce Posner^a, Deepak Nijhawan^a, and Joseph M. Ready^{a,*}

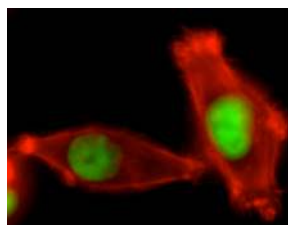
^aDepartment of Biochemistry, UT Southwestern Medical Center, 5323 Harry Hines Blvd, Dallas, Texas, 75390-9038

^bDepartment of Internal Medicine, UT Southwestern Medical Center, 5323 Harry Hines Blvd, Dallas, Texas, 75390-9038

Abstract

Polycyclic tetrahydroxanthones comprise a large class of cytotoxic natural products. No mechanism of action has been described for any member of the family. We report the synthesis of kibelone C and several simplified analogs. Both enantiomers of kibelone C show low nM cytotoxicity towards multiple human cancer cell lines. Moreover, several simplified derivatives with improved chemical stability display higher activity than the natural product itself. In vitro studies rule out interaction with DNA or inhibition of topoisomerase, both of which are common modes of action for polycyclic aromatic compounds. However, cellular studies reveal that kibelone C and simplified derivatives disrupt the actin cytoskeleton without directly binding actin or affecting its polymerization in vitro.

Graphical abstract



Introduction

Kibelones A-C (Scheme 1, **1–3**) are members of a growing class of natural products characterized by a hexacyclic, polyaromatic scaffold and a tetrahydroxanthone moiety.^{1,2} These microbial metabolites arise biosynthetically from multiple cyclizations from a single

* *Corresponding Author.* joseph.ready@utsouthwestern.edu.

ASSOCIATED CONTENT

Supporting Information

The Supporting Information is available free of charge on the ACS Publications website. Synthetic procedures, characterization data, supplementary figures (PDF)

The authors claim no competing financial interests.

polyacetate chain, accounting for the high degree of oxygenation on the aromatic and heteroaromatic rings.³ Structurally related natural products include simaomicin α ,⁴ actinoplanone,⁵ SCH-56036⁶ and kigamicin A.⁷ Additionally, natural products such as cervinomycin A2⁸ and FD-594⁹ feature aromatic F-rings as part of a xanthone moiety. All of these secondary metabolites share a common hexacyclic core structure and differ with regard to the substitution pattern on the aryl and heteroaryl rings. They display potent cytotoxicity, although no mechanism of action has been elucidated for any member of the family. In particular, they generally show broad-spectrum toxicity including anti-cancer, antibiotic and anti-fungal activity. Simaomicin α has shown activity preventing coccidiosis in chickens,^{4b} and was found to induce G1 arrest in cultured cancer cells.^{4c} Likewise, the kigamicins have demonstrated efficacy in inhibiting tumor growth in immunocompromised mice.^{7c} Despite these promising biological activities, little is understood regarding the mechanism by which polycyclic tetrahydroxanthone natural products kill microbial and mammalian cells.

The Capon group discovered the kibelones in the culture media of a soil actinomycete *Kibdelosporangium* sp.^{1,10} Extensive 1- and 2-dimensional NMR data revealed the presence of a chlorinated isoquinolinone AB ring system. The DEF ring tetrahydroxanthone included three stereogenic hydroxyl groups with the relative stereochemistry shown in Scheme 1. The three congeners vary at the oxidation state of the B ring (quinone vs. hydroquinone) and the C ring (saturated vs. unsaturated). Furthermore, the isolation group revealed that kibelone C could spontaneously oxidize to kibelones A and B under aerobic conditions.

The kibelones displayed potent cytotoxicity against a panel of human cancer cell lines. All three compounds arrested growth of cell lines derived from lung, colon, ovarian, prostate, breast and other tumor types with GI₅₀'s < 5 nM. They additionally showed robust toxicity towards *B. subtilis* bacteria. It is unclear if the kibelone A-C are in fact equally active or if they interconvert under the conditions of the biological assays. The NCI COMPARE analysis did not reveal a strong correlation between the toxicity profile of the kibelones and that of other known cytotoxins, indicating that they might operate through an unknown mode of action.

The combination of unique structural features and compelling biological properties make the polycyclic xanthone natural products attractive targets for total synthesis.² The Kelly group described the first synthesis of the xanthone-containing natural product cervinomycins A1 and A2,¹¹ and reports from the Rao and Mehta groups followed shortly thereafter.^{12,13} The Suzuki group made an important contribution to the area with a synthesis of FD-594 aglycone; theirs was the first enantioselective synthesis of a member of the family.¹⁴ The Porco group reported an elegant synthesis of the naturally occurring (+)-kibelone C,¹⁵ and we described a synthesis of (-)-simaomicin α in 2013.¹⁶ More recently, the Martin group recently described a total synthesis of the aglycone of IB-00208.¹⁷ Additionally, several groups have reported synthetic studies towards natural products of the hexacyclic xanthone family.¹⁸

We set as an initial objective the development of a flexible and enantioselective synthetic route that could provide access to the natural product and allow assignment of the absolute stereochemistry of **1–3**.¹⁹ Based on initial biological results described below, we then

pursued simplified analogues of the kibelones. Here we describe the evolution of our synthetic strategy, the synthesis of simplified analogues maintaining full biological activity, and initial efforts to understand the mode of action of the kibelones.

Results and Discussion

Synthetic strategy

In considering a synthetic approach to the kibelones and related natural products, we targeted the C5–C6 bond that connects the B and D rings (Scheme 2). Strategically, retrosynthetic disconnection of this bond would deconstruct the C-ring to suggest an intermediate such as diaryl alkyne **10** in which the isoquinoline and tetrahydroxanthone moieties can be viewed as independent ring systems. From a tactical perspective, we were attracted to a late-stage C5–C6 bond construction because multiple methods exist for the formation of biaryl bonds including cross-coupling, oxidative coupling and C-H functionalization reactions. Finally, we reasoned that the isoquinolinone fragment **11** could be joined to tetrahydroxanthone subunit **12** using an equivalent of acetylene as a lynchpin.

Fragment synthesis

To prepare the isoquinolinone AB rings, we explored cyclization of aryl aldehyde **15** (Scheme 3). To this end, amino alcohol **13**²⁰ was coupled to the acid chloride derived from benzoic acid **14**.²¹ Subsequent oxidation generated the cyclization substrate, aldehyde **15**. Both BCl₃ and BBr₃ promoted electrophilic addition to yield a benzylic alcohol (not shown), which could be dehydrated to yield isoquinolinone **16** under acidic conditions. While BCl₃ only demethylated the phenol ortho to the amide, BBr₃ yielded doubly demethylated material. It is unclear if demethylation is required for cyclization, but we note that we never observed cyclized products that retained both methyl groups. Moreover, the highest yields were obtained when the BCl₃ was added in two portions – 1 equiv followed by 1.5 equiv. Monitoring of a reaction in CDCl₃ by ¹H NMR revealed that the first equivalent of BCl₃ completely consumed aldehyde **15** to form an intermediate we characterized as a chlorohydrin.²² Subsequent addition of the remaining 1.5 equiv BCl₃ resulted in demethylation and cyclization. By contrast, the starting material was recovered largely intact following exposure to TiCl₄, Sc(OTf)₃, AlCl₃ and ZnCl₂. Following cyclization with BBr₃, an acetylene equivalent was introduced using a Sonogashira coupling to provide terminal alkyne **17**.²³

Synthesis of the tetrahydroxanthone subunit started with preparation of the D-ring. Formylation of phenol **18**²⁴ was anticipated to introduce the xanthone carbonyl. However, reaction with formaldehyde under Lewis acid conditions proved unsatisfactory (Table 1, entry 1).²⁵ Phenol **18** was completely consumed, and the crude reaction mixtures were remarkably clean. Nonetheless, isolated yields remained under 50% under a variety of temperature and concentration profiles. We speculate that the benzylic alcohol intermediate formed under the reaction conditions (**21**, or corresponding metal alkoxide) might have eliminated water to form the quinone methide **24**, which might have undergone polymerization. Alternative formylating agents such as methoxydichloromethane (entry 2) or tetraazaadamantane (**23**, entry 3) provided poor regioselectivity and/or low yields.²⁶ A

MOM-ether, **19**, could be cleanly lithiated, but as shown in entry 4, trapping with dimethylformamide or CO₂ was not successful. Finally, we discovered that aluminum-based Lewis acids generated the benzylic alcohol **21** cleanly and in high yield (entry 5).²⁷ Subsequent protection of **21** with MOM-Cl under phase transfer conditions and oxidation gave the desired aldehyde **25** (eq 1).

Our synthesis of the F-ring took advantage of pseudo-C₂ symmetry of the F ring that related the C11 and C13 hydroxyl groups and the C10 and C14 oxygenation. In this endeavor, we were inspired by Myers' use of the Shi epoxidation to form trans-diols.^{28,29} Specifically, resorcinol was silylated and reduced with sodium and ammonia to provide the known bis-enol ether **26**.²⁸ Epoxidation with the Shi catalyst (**27**) was followed by immediate reduction with borane to provide the doubly protected tetraol **30** as a single observed diastereomer and enantiomer.³⁰ This reaction installed the C11 and C13 alcohols with the correct relative stereochemistry for the kibdelones. Additionally, it introduced the required oxygenation at C10 and C14. As proposed by Myers, borane presumably acts as a Lewis acid to promote ring-opening of the silyloxyoxirane (see **29**); intramolecular hydride delivery yields the protected diol. Selective mono-tosylation of **30** came as a welcome surprise. Analysis of ¹H-¹H coupling constants for **31** suggested a trans-diaxial orientation of the large TBS and tosyl groups. This conformation places the remaining OH in an equatorial position as shown. Steric hindrance from the adjacent OTBS group may prevent reaction with a second equivalent of TsCl. Next, the C10 hydroxyl was oxidized under basic conditions, which resulted in β-elimination of the tosyl group to yield the enone **32**. Finally, iodination and Luche reduction of the enone completed the synthesis of the F-ring iodide **33**.

With access to an appropriate F-ring vinyl iodide, we attempted to join it to the D-ring and construct the tetrahydroxanthone (Scheme 5). In preliminary studies, we were unable to effect carbonylative coupling of aryl stannane **34** with variously protected F-ring precursors (**35**, eq 2). Likewise, fully protected F-ring subunits could be metalated, but we observed no addition to the hindered and electron-rich D-ring aldehyde (eq 3). Ultimately, Li and Nicolaou's synthesis of diversanol proved informative.³¹ Thus, we speculated that the C10 protecting group might be causing steric crowding during the addition. Accordingly we deprotonated **33** with MeLi and then converted it to the vinyl lithium with *n*-BuLi. Addition to aldehyde **25** then yielded the benzylic alcohol **40** as an inconsequential mixture of diastereomers. (eq 4).

To synthesize the tetrahydroxanthone subunit, diol **40** was oxidized under Dess-Martin conditions to an unstable diketone (Scheme 6). This material was immediately exposed to perchloric acid in a mixed solvent system containing acetone and *tert*-butanol to form the tricyclic tetrahydroxanthone **42**.³⁰ This cyclization may involve intramolecular conjugate addition of acetone hemiketal **41** to install the acetonide and set the correct C10 stereochemistry. When the cyclization was performed in the absence of acetone, the triol **43** was formed as a mixture of C10 diastereomers. Likewise, when *tert*-butanol was excluded from the reaction mixture, the methylene ketal **44** was formed, presumably from the formaldehyde liberated during MOM deprotection.

Synthesis of *ent*-Kibdelone C

The isoquinolinone fragment was linked to the tetrahydroxanthone using a Cu-free Pd coupling.³² Even in the absence of copper salts, rigorous degassing and slow addition of the alkyne was required to avoid oxidative coupling to form a diyne side products. Hydrogenation and Cu-catalyzed iodination³³ yielded the phenol **46**, which could be treated with (Boc)₂O to form the carbonate **47**. An intramolecular, Pd-mediated C-H arylation reaction formed the C4–C5 biaryl bond and constructed the C-ring of the natural product.³⁴ This transformation required extensive optimization, which revealed that the OBoc group, the Pd source, the temperature and the sodium pivalate buffer were all important. The free phenol **46** or methyl ether **48** only generated trace amounts of desired product, while the methoxyethoxy methyl (MEM) containing substrate **49** gave around 15% of the desired product. The success of the MEM and Boc-containing substrates indicate that these groups may coordinate to and stabilize the Pd(II) center within an aryl palladium iodide intermediate. In this cyclization, Pd(OAc)₂ was effective, but more Lewis acidic Pd(II) salts [e.g. PdCl₂, Pd(TFA)₂, Pd(OTf)₂] caused aromatization of the F-ring. Likewise, at temperatures below 85 °C, only deiodination was observed whereas at temperatures higher than 95 °C, extensive decomposition occurred. Finally, in situ generation of NaOPiv facilitated C-H functionalization, presumably through a concerted metalation-deprotonation as proposed by Fagnou and coworkers.³⁵

Access to the full kibdelone carbon skeleton allowed us to prepare the natural product and several simple derivatives. Thus, halogenation with **51** introduced the A-ring chloride, albeit with an unexpected complication. Specifically, the desired chloroisoquinolinone was accompanied by side products that we tentatively characterized as the hydration products (see **52**). Multiple stereoisomeric halohydrins were thus formed, and all of the products were generated as ~1:1 mixtures of atropisomers due to hindered rotation around the C4–C5 bond. Accordingly, no purification was possible at this stage. Next, treatment with HClO₄ removed the Boc group and the acetonide and prompted dehydration of the A-ring back to the isoquinolinone. However, only about half of the C13 MOM group was removed, generating similar amounts of diols **53** and **54**. Efforts to increase conversion led to decomposition. Moreover, some of the formaldehyde (or its equivalent) that formed during removal of the MOM group was trapped by the C10–C11 diol to yield the methylene ketal **55**. This mixture of products was then treated with PhI(OAc)₂ to remove the B-ring methyl group. Finally, exposure to BCl₃ cleaved the D-ring methyl group and any remaining MOM or methylene ketal. Reductive workup converted the C-ring quinone to the hydroquinone, and completed the synthesis of kibdelone C. The natural product was prone to oxidation, as had been reported by the isolation group. Accordingly, the final product was purified by HPLC, immediately lyophilized, and handled under an inert atmosphere.¹⁹

The specific rotation of synthetic kibdelone (–40) was similar in magnitude but opposite in sign to the naturally occurring material (+47). This observation indicated that our synthetic material was enantiomeric to the natural product, a conclusion consistent with contemporaneous results from the Porco group.^{15b}

Synthesis and evaluation of intitial derivatives of kibelone C

We repeated the sequence shown above except for the use of the enantiomeric Shi catalyst³⁶ (*ent*-**27**) to provide the natural enantiomer for side-by-side comparison of their biological potencies (see below).²² Additionally, our synthetic scheme allowed us to prepare two simple analogs to test the requirements for biological activity. In particular, omitting the oxidative removal of the B-ring methyl group yielded methyl-kibelone C (**57**). As anticipated, this compound was much more stable than the natural product, with no observed oxidative conversion to the B-ring hydroquinone under ambient conditions. Similarly, intermediate **50** was chlorinated and deprotected under acidic conditions; low-temperature treatment with BCl₃ retained both the B-ring and innerrim D-ring methoxy groups to yield dimethyl kibelone C (**56**) as a 1:1 mixture of atropisomers.

The syntheses of both enantiomers of kibelone C and methyl kibelone C allowed us to answer two initial questions. Is the absolute configuration of the natural product important for biological activity? And is a quinone required for biological activity? Concerning the latter question, the Kapon group had observed rapid aerobic oxidation of kibelone C to kibelones A (**1**) and B (**2**), which feature quinone moieties. Moreover, they reported nearly identical cytotoxicity with the 3 congeners. Since quinones are reactive to nucleophiles and can act as electron acceptors, we wondered if a quinone might be required for biological activity (eq 2). In this scenario, kibelone C would act as a pro-drug, undergoing oxidation under the assay conditions. Of relevance to this question, we noted the increased aerobic stability of methyl kibelone C, which appeared to be indefinitely stable under ambient conditions. It provided a control compound that would be less prone to generate quinones compared to the naturel product. We therefore tested the cytotoxicity of both enantiomers of kibelone C and methyl kibelone C (**57**) against the colon cancer cell line HCT116. As shown in Fig 1, the four compounds showed potent toxicity with overlapping dose-response curves. The concentration that resulted in 50% less viability compared to DMSO control (IC₅₀) was calculated for each compound. The calculated IC₅₀'s were between 3 and 5 nM under these assay conditions. From these data we conclude that a) the absolute configuration of the natural product does not affect activity, and b) quinone formation is likely not required for biological activity.³⁷

F-ring derivatives of kibelone C

The equivalent cytotoxicity of (+)- and (-)-kibelone C is consistent with our recent discovery that the unnatural enantiomer of simaomicin α shows potent cytotoxicity towards human cancer cell lines (3 lines, IC₅₀ < 100 nM). Of note, Porco and coworkers previously found that kibelone derivatives lacking an F-ring were >1000-fold less active than the natural product.³⁶ These observations prompted us to prepare analogs of kibelone C featuring simplified F-rings to determine the requirements for activity (Scheme 7). Towards that end, iodo-cyclohexenols **58** and **59** were lithiated and exposed to aldehyde **25**. Subsequent Dess-Martin oxidation and treatment with perchloric acid yielded the tetrahydroxanthones that lack oxygenation at C11 (**61**) or C11 and C13 (**60**, Scheme 7a). As an alternative to the acid-induced cyclization, enone **62** was treated with HCl to remove the MOM group (**63**). Oxidative cyclization involving SeO₂ provided modest yields of the diol **64**, which lacks an alcohol at C13 (Scheme 7b).³⁸

The alcohols of **60** and **61** were protected, which allowed separation of the cis and trans diastereomeric diols **66** (Scheme 7c). Separately, these aryl bromides were coupled with alkyne **17** under Cu-free conditions to yield the diaryl alkynes **67–68**.³¹ Hydrogenation of the alkyne proceeded in the presence of the benzyl and BOM groups. Next, C4 was iodinated under our Cu-catalyzed conditions, and the B-ring phenol was converted to a carbonate. Iodide **69**, featuring only one alkoxy substituent on the F-ring, was cyclized in the presence of Pd(OAc)₂, PCy₃, and NaOPiv. This C-H arylation reaction formed the C-ring and completed the carbon skeleton to provide hexacycle **71**. Likewise, *trans*-**70** reacted cleanly under the same reaction conditions to provide the hexacyclic product *trans*-**72** in an excellent 86% yield. By contrast, the cis diastereomer, *cis*-**70**, generated the tetrahydroxanthone *cis*-**72** in only 43% yield. The reaction additionally provided the xanthone **73** containing a fully aromatic F ring. This side product arose from elimination of the benzyl and BOM ethers. Finally, removal of the benzyl, BOM and Boc groups and the D-ring methyl of intermediates **71–73** gave the deprotected analogs of kibelone C. Both the *cis*-**72** and *trans*-**72** diastereomers produced the same ~1:1 ratio of diol **76** under the acidic deprotection conditions. Using the same synthetic strategy, di-benzyl ether **64** was advanced to diol **77**, which lacks the C13 hydroxyl of kibelone (Scheme 7d).²² Of note, each of these analogs also differs from kibelone by the absence of the A-ring chloride and the presence of the B-ring methoxy group.

Several synthetic analogs were tested for biological activity against three non-small cell lung cancer cell lines that have been shown to display differential sensitivity to various cytotoxins.³⁹ Each cell line was treated with each compound in a 12-point dose-response experiment in triplicate ranging from 50 μ M to 30 pM. Cell viability was measured with CellTiter-Glo® (Promega, Inc.) after four days in culture at 37 °C. The IC₅₀ values are shown in Table 2. As described above, kibelone C and methyl-kibelone (**57**) showed low-nM toxicity. By contrast, dimethyl-kibelone **56**, which retains a methyl group on the convex D-ring phenol, lost >100-fold potency. Excitingly, diol **76**, which features the same F-ring as simaomicin α , showed IC₅₀ values less than 5 nM, as did diol **77**, which lacks the C13 hydroxyl. The analog **75** retains only the C10 hydroxyl, but was as active as the natural product. Finally, the simplest analog, **74**, with an unsubstituted aryl F-ring, was likewise as active as kibelone C. Taken together, the data show that hydroxylation on the F-ring, chlorination, and a B-ring hydroquinone are not required for activity. Therefore, simplified achiral and racemic analogs maintain full cytotoxic activity, which could facilitate studies to understand their mechanism of action.

Biological Studies

Kibelone does not bind DNA

Molecular models of kibelone C revealed a helical topology of the largely planar ring system. This architecture suggested the possibility that kibelone C and derivative might interact with nucleic acids and/or nucleic acid-binding proteins. Indeed, polycyclic aromatic molecules can intercalate into DNA, and this activity often underpins their cytotoxicity.⁴⁰ To determine if intercalation into DNA was responsible for the cell killing associated with kibelone, we attempted to rescue cells from kibelone by adding exogenous DNA. In this

experiment, the added DNA would compete with cellular DNA for binding to drug, thereby resulting in a rightward shift in the dose-response curve. As a positive control, H2122 non-small cell lung cancer cells were treated with varying concentrations of actinomycin, an anti-cancer agent known to bind DNA and inhibit transcription.⁴¹ In the absence of added DNA, actinomycin displayed an IC₅₀ of 0.5 nM.⁴² However, the IC₅₀ value shifted to 51 nM in the presence of 40 µg of herring sperm DNA (Table 3). By contrast, paclitaxel, which does not bind DNA and served as a negative control, displayed equivalent IC₅₀ values in the presence and absence of added DNA (6 nM). In the key experiment, adding exogenous DNA to the cell cultures had no impact on the toxicity of *ent*-kibdelone C. We interpret this result to indicate that kibdelone's mechanism of action does not involve binding to DNA.

Kibdelone does not inhibit topoisomerase

Several polycyclic, cytotoxic natural products inhibit topoisomerase, offering a potential mechanism for the toxicity observed with the kibdelone family of cytotoxins.⁴³ To explore this possibility, methyl kibdelone C (**57**) was incubated with topoisomerase I and supercoiled DNA (Sc DNA). Topoisomerase I relaxes supercoiled DNA by introducing single-strand DNA breaks, allowing the cleaved strand to unwind, and rejoining the DNA fragments. As shown in Fig 2a, Sc DNA (lane 1) is readily relaxed to a series of topoisomers in the absence of methyl kibdelone C (lane 6), and this activity is not affected by up to 10 µM compound (lanes 7–11). While topoisomerase I induces single strand DNA breaks, topoisomerase II creates double-strand breaks. This activity can be assayed using catenated kinetoplast DNA (kDNA), a series of interlocked circles of DNA (Fig 2b, lane 1). This high molecular weight complex can be decatenated with topoisomerase II to generate circular DNA (lane 2). While etoposide was found to interfere with this process by generating linear DNA fragments (lanes 3, 4), methyl kibdelone C again had no effect on enzymatic activity or product distribution up to 10 µM (lanes 6–11). We conclude that the kibdelone family of compounds does not inhibit either topoisomerase I or II.

Kibdelone and derivatives affect the cytoskeleton

Kibdelone C and its active derivatives caused morphological changes to human cancer cells including cell contraction followed by cell death within 24 h. To study this activity in more detail, HeLa cells were cultured in the presence of DMSO or various cytotoxins. After 12h, cells were fixed and stained with DAPI to mark the nuclei and with an F-actin marker (FITC-phalloidin or Alexa448-phalloidin) to observe the cytoskeleton. As shown in Fig 3a, DMSO-treated cells displayed an oval-shaped nucleus and diffuse actin cytoskeleton. Cell membranes featured cortical actin structures as expected. By contrast, *ent*-kibdelone C [(–)–**3**] resulted in contraction of the cells and the formation of actin fibers. Specifically, 7% of untreated cells contained these stress fibers whereas greater than 60% of cells treated with 50 nM kibdelone C featured these structures after 12h (Fig 3A, B; quantification in Fig S5). The formation of stress fibers appears to be associated with the tetrahydroxanthone family of natural products and is not a general property of cytotoxins. For example, simaomicin **a** caused an identical phenotype (Fig 3D), as did the active analogs described above (Fig S6). As shown in Fig S6, simplified analogs **57**, **76** and **77** showed similar cell contraction/rounding and stress fiber formation as the natural products themselves. Two representative anti-cancer drugs did not cause actin stress fibers to form. For example, bortezomib, a

proteasome inhibitor, instead led to cell rounding without nuclear disruption. Paclitaxel, a microtubule stabilizing agent, created disorganized nuclei and cell rounding (Fig 3E, F). This comparison indicates that the stress fibers and morphological effects are not general activities associated with cell death. Rather, they appear to be specific to the mode of action of the cytotoxic tetrahydroxanthones.

Having observed effects on the actin cytoskeleton, we considered whether kibelone C might directly affect actin polymerization. To assess this possibility, actin was polymerized *in vitro* in the absence or presence of kibelone C. This assay involves incorporation of tracer quantities of pyrene-labeled actin into growing actin filaments, which provides a fluorescent readout of polymerization.⁴⁴ Individual time-course traces are shown in Fig 4, and they demonstrate that actin polymerization is not affected by up to 100 nM kibelone C. The inset shows the average relative rates of polymerization in the presence or absence of kibelone C ($n = 3$), again indicating no effect. Taken together, the data suggests that kibelone and related compounds affect the actin cytoskeleton, but this effect does not involve a direct interaction with kibelone.⁴⁵

Conclusions

A convergent total synthesis of kibelone C allowed access to several derivatives of the natural product. Substituents around the convex periphery appear to have little impact on the biological activity. Thus, the methyl and propyl groups of the isoquinolinones of simaomicin α and kibelone C both lead to potent toxicity. Similarly, the chloride of the latter natural product is dispensable. The B-ring can tolerate a cyclic ketal as in simaomicin α , phenol as in kibelone C, or a methoxy group as in several synthetic derivatives. Similarly, the hydroxylation around the F-ring is apparently not required for activity. Both enantiomers of kibelone C and simaomicin α are active, as are analogues missing the C11 and/or C13 hydroxyls. Most surprising, an aryl F ring lacking hydroxylation was fully active. By contrast, the hydroxyls on the concave portion of the natural product appear critical, as shown by the substantial loss in activity associated with dimethyl ether **56**. Prior studies showed that the EF rings of the tetrahydroxanthone are indispensable.³⁶ These results suggest that the polycyclic ring system may essentially act as scaffolding to present the A- and E-ring carbonyls and B- and D-ring phenols in a defined orientation. It is perhaps noteworthy that all of the natural products shown in Scheme 1 share this functionality. This common structure could suggest a similar biological mechanism for these natural products. Moreover, it seems plausible to envision a role for metal binding by the phenols common the B and D rings of the tetrahydroxanthone natural products, but that possibility remains speculative at present.

Our initial studies ruled out common modes of activity – DNA binding and topoisomerase. Cell imaging displayed profound changes to the actin cytoskeleton, but *in vitro* studies showed no direct effect on actin polymerization. These data indicate that the kibelones must be acting upstream of actin regulation. The structural requirements for activity and the simplified derivatives described here should facilitate the discovery of tools to identify the direct binding partners for these cytotoxins.

Supplementary Material

Refer to Web version on PubMed Central for supplementary material.

Acknowledgments

Financial support from the Welch Foundation (I-1612), CPRIT (RP101016) and the NIH (R01 GM102403). We appreciate assistance from Dr. Luke Rice with in vitro tubulin polymerization assays, from Yingli Duan culturing cancer cells, and from Lynda Doolittle with actin polymerization assays.

REFERENCES

1. Ratnayake R, Lacey E, Tennant S, Gill JH, Capon RJ. *Chem. Eur. J.* 2007; 13:1610–1619. [PubMed: 17091523]
2. Winter DK, Sloman DL, Porco JA Jr. *Nat. Prod. Rep.* 2013; 30:382–391. [PubMed: 23334431]
3. Carter GT, Goodman JJ, Torrey MJ, Borders DB, Gould SJ. *J. Org. Chem.* 1989; 54:4321–4323.
4. (a) Lee TM, Carter GT, Borders DB. *J. Chem. Soc. Chem. Commun.* 1989:1771–1772. (b) Maiese WM, Korshalla J, Goodman J, Torrey MJ, Kantor S, Labeda DP, Greenstein M. *J. Antibiotics.* 1990; 43:1059–1063. [PubMed: 2211367] (c) Koizumi Y, Tomoda H, Kumagai A, Zhou X-p, Koyota S, Sugiyama T. *Cancer Sci.* 2009; 100:322–326. [PubMed: 19077005]
5. Kobayashi K, Nishino C, Ohya J, Sato S, Mikawa T, Shiobara Y, Kodama M. *J. Antibiotics.* 1988; 41:502–511. [PubMed: 3372357]
6. Chu M, Truumees I, Mierzwa R, Terracciano J, Patel M, Das PR, Puar MS, Chan T-M. *Tetrahedron Lett.* 1998; 39:7649–7652.
7. (a) Kunimoto S, Lu J, Esumi H, Yamazaki Y, Kinoshita N, Honma Y, Hamada M, Ohsono M, Ishizuka M, Takeuchi T. *J. Antibiotics.* 2003; 56:1004–1011. [PubMed: 15015727] (b) Kunimoto S, Someno T, Yamazaki Y, Lu J, Esumi H, Naganawa H. *J. Antibiotics.* 2003; 56:1012–1017. [PubMed: 15015728] (c) Lu J, Kunimoto S, Yamazaki Y, Kaminishi M, Esumi H. *Cancer Sci.* 2004; 95:547–552. [PubMed: 15182438]
8. Nakagawa A, Omura S, Kushida K, Shimizu H, Lukacs G. *J. Antibiotics.* 1987; 40:301–308. [PubMed: 3570983]
9. Qiao Y-F, Okazaki T, Ando T, Mizoue K, Kondo K, Eguchi T, Kakinuma K. *J. Antibiotics.* 1998; 51:282–287. [PubMed: 9589063]
10. Ratnayake R, Lacey E, Tennant S, Gill JH, Capon R. *J. Org. Lett.* 2006; 8:5267–5270.
11. Kelly TR, Jagoe CT, Li Q. *J. Am. Chem. Soc.* 1989; 111:4522–4524.
12. Rao AVR, Yadav JS, Reddy KK, Upender V. *Tetrahedron Lett.* 1991; 32:5199–5202.
13. Mehta G, Shah SR, Venkateswarlu Y. *Tetrahedron.* 1994; 50:11729–11742.
14. Masuo R, Ohmori K, Hintermann L, Yoshida S, Suzuki K. *Angew. Chem. Int. Ed.* 2009; 48:3462–3465.
15. (a) Sloman DL, Mitasev B, Scully SS, Beutler JA, Porco JA. *Angew. Chem. Int. Ed.* 2011; 50:2511–2515. (b) Sloman DL, Bacon JW, Porco JA. *J. Am. Chem. Soc.* 2011; 133:9952–9955. [PubMed: 21648477]
16. Wang Y, Wang C, Butler JR, Ready JM. *Angew. Chem. Int. Ed.* 2013; 52:10796–10799.
17. (a) Yang J, Knueppel D, Cheng B, Mans D, Martin SF. *Org. Lett.* 2015; 17:114–117. [PubMed: 25513888] (b) Knueppel D, Yang J, Cheng B, Mans D, Martin SF. *Tetrahedron.* 2015; 71:5741–5757. [PubMed: 26273110]
18. (a) Duthaler RO, Heuberger C, Wegmann UHU, Scherrer V. *Chimia.* 1985; 39:174–182. (b) Walker ER, Leung SY, Barrett AGM. *Tetrahedron Lett.* 2005; 46:6537–6540. (c) Xiao Z, Cai S, Shi Y, Yang B, Gao S. *Chem. Commun.* 2014; 50:5254–5257.
19. Butler JR, Wang C, Bian J, Ready JM. *J. Am. Chem. Soc.* 2011; 133:9956–9959. [PubMed: 21648478]
20. Johansson, R.; Karlstroem, S.; Kers, A.; Nordvall, G.; Rein, T.; Slivo, C. International Patent. WO 039139 A1. 2008.

21. Barfknecht CF, Nichols DE. *J. Med. Chem.* 1971; 14:370–372. [PubMed: 5553756]
22. See supporting information for details.
23. Hundertmark T, Littke AF, Buchwald SL, Fu GC. *Org. Lett.* 2000; 2:1729–1731. [PubMed: 10880212]
24. Yonezawa S, Komurasaki T, Kawada K, Tsuru T, Fuji M, Kugimiya A, Haga N, Mitsumori S, Inagaki M, Nakatani T, Tamura Y, Takechi S, Taishi T, Ohtani M. *J. Org. Chem.* 1998; 63:5831–5837. [PubMed: 11672184]
25. Casiraghi G, Casnati G, Puglia G, Sartori G, Terenghi G. *J. Chem. Soc. Perkin 1.* 1980:1862–1865.
26. Blazevic N, Kolbah D, Belin B, Sunjic V, Kajfez F. *Synthesis.* 1979:161–176.
27. Bigi F, Casiraghi G, Casnati G, Sartori G, Gasparri Fava G, Ferrari Belicchi M. *J. Org. Chem.* 1985; 50:5018–5022.
28. Lim SM, Hill N, Myers AG. *J. Am. Chem. Soc.* 2009; 131:5763–5765. [PubMed: 19341239]
29. Shi Y. *Accts. Chem. Res.* 2004; 37:488–496.
30. The e.r. of tetraol **30** was determined from the bis-Mosher's ester as described in ref 28.
31. Nicolaou KC, Li A. *Angew. Chem. Int. Ed.* 2008; 47:6579–6582.
32. Soheili A, Albaneze-Walker J, Murry JA, Dormer PG, Hughes DL. *Org. Lett.* 2003; 5:4191–4194. [PubMed: 14572282]
33. (a) This iodination was discovered serendipitously when a sample of the reduction product of **45** containing Cu salts (from a failed attempt at Cu-promoted phenolic coupling cyclization) was exposed to *N*-iodosuccinimide. For Cu-catalyzed bromination and chlorination of arenes, see Yang L, Lu Z, Stahl SS. *Chem. Commun.* 2009:6460–6462. (b) Iodination as a side-product: Li X, Hewgley JB, Mulrooney CA, Yang J, Kozlowski MC. *J. Org. Chem.* 2003; 68:5500–5511. [PubMed: 12839440] (c) Cu(OH)Cl • TMEDA: Nakajima M, Miyoshi I, Kanayama K, Hashimoto S-i, Noji M, Koga K. *J. Org. Chem.* 1999; 64:2264–2271.
34. Seminal contributions on C-H arylation: Hennings DD, Iwasa S, Rawal VH. *J. Org. Chem.* 1997; 62:2–3. [PubMed: 11671356] Ackermann L, Vicente R, Kapdi AR. *Angew. Chem. Int. Ed.* 2009; 48:9792–9826. Gutekunst WR, Baran PS. *Chem. Soc. Rev.* 2011; 40:1976–1991. [PubMed: 21298176]
35. Campeau L-C, Parisien M, Jean A, Fagnou K. *J. Am. Chem. Soc.* 2005; 128:581–590. [PubMed: 16402846]
36. Zhao M-X, Shi Y. *J. Org. Chem.* 2006; 71:5377–5379. [PubMed: 16808531]
37. Winter DK, Endoma-Arias MA, Hudlicky T, Beutler JA, Porco JA. *J. Org. Chem.* 2013; 78:7617–7626. [PubMed: 23834060]
38. Chan K-F, Zhao Y, Chow LMC, Chan TH. *Tetrahedron.* 2005; 61:4149–4156.
39. (a) For cytotoxicity screening against several NSCLC lines including the ones used here, see data generated by the Cancer Target Discovery and Development (CTD₂) Network (<https://ctd2.nci.nih.gov/dataPortal/>) established by the National Cancer Institute's Office of Cancer Genomics. Theodoropoulos PC, Gonzales SS, Winterton SE, Rodriguez-Navas C, McKnight JS, Morlock LK, Hanson JM, Cross B, Owen AE, Duan Y, Moreno JR, Lemoff A, Mirzaei H, Posner BA, Williams NS, Ready JM, Nijhawan D. *Nat. Chem. Biol.* 2016; 12:218–225. [PubMed: 26829472]
40. (a) K Prasad KS, Nayak R. *FEBS Letters.* 1976; 71:171–174. (b) Shafer RH, Burnette RR, Mirau PA. *Nucleic Acids Res.* 1980; 8:1121–1132. [PubMed: 7443543] (c) Van Dyke M, Dervan P. *Science.* 1984; 225:1122–1127. [PubMed: 6089341]
41. Sobell HM. *Proc. Natl. Acad. Sci.* 1985; 82:5328–5331. [PubMed: 2410919]
42. Warnick-Pickle DJ, Byrne KM, Pandey RC, White RJ. *J. Antibiotics.* 1981; 34:1402–1407. [PubMed: 7319903]
43. (a) Latham MD, King CK, Gorycki P, Macdonald TL, Ross WE. *Cancer Chemother. Pharm.* 1989; 24:167–171. (b) Capranico G, Ferri F, Fogli MV, Russo A, Lotito L, Baranello L. *Biochimie.* 2007; 89:482–489. [PubMed: 17336444]
44. Doolittle LK, Rosen MK, Padrick SB. *Methods Mol. Biol.* 2013; 1045:273–293. [PubMed: 23868594]

45. Kibdeleone C also does not affect the polymerization of tubulin, another common target of cytotoxic natural products. See Figure S8.

Author Manuscript

Author Manuscript

Author Manuscript

Author Manuscript

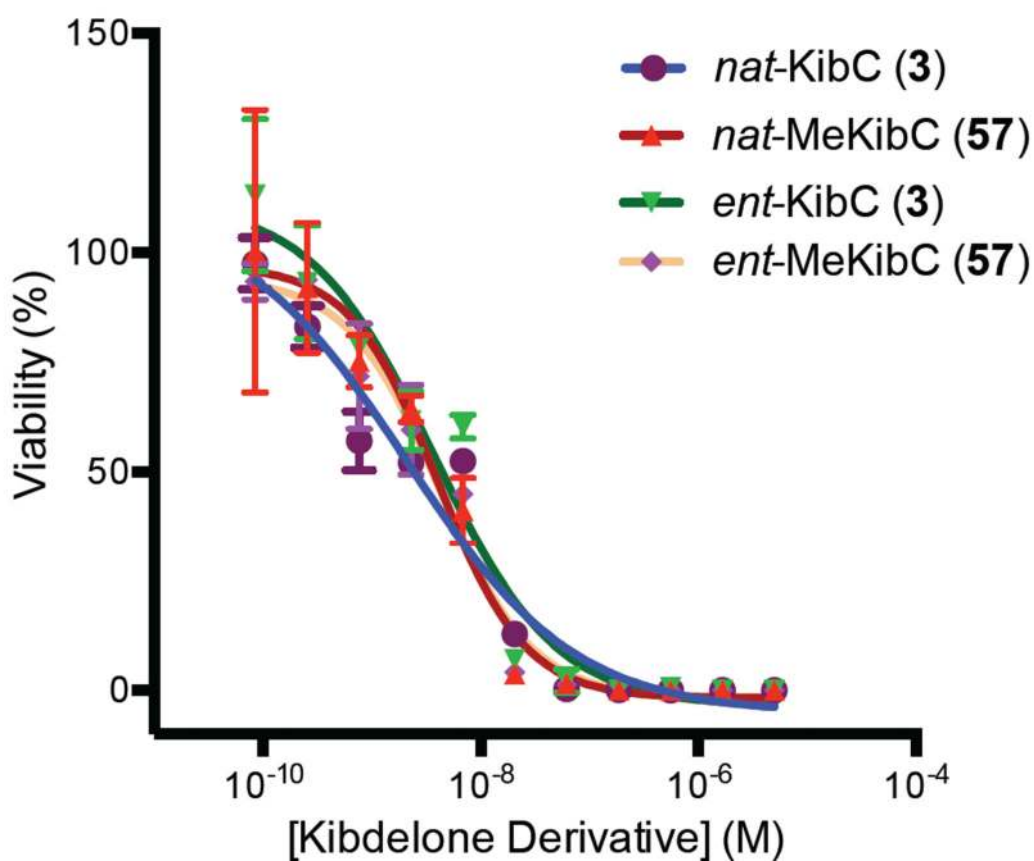
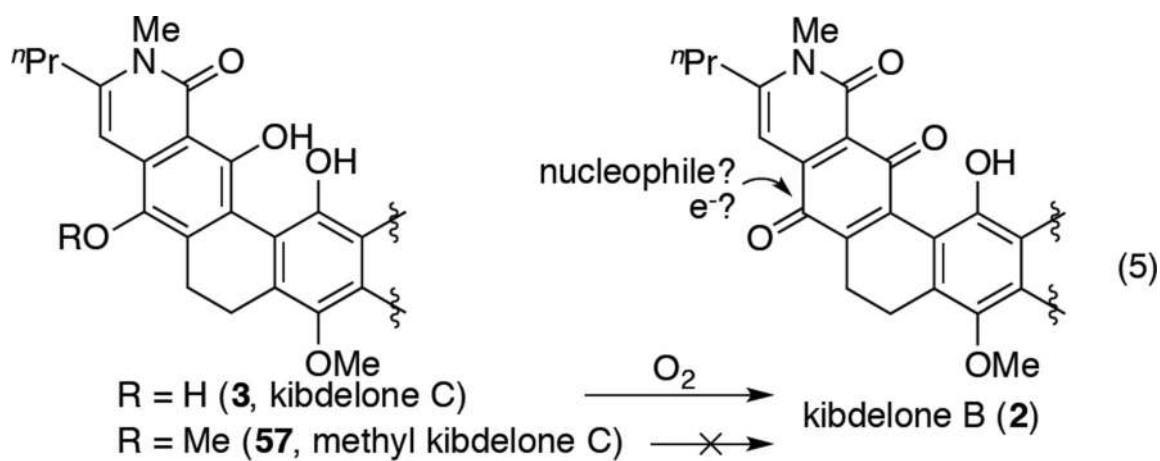
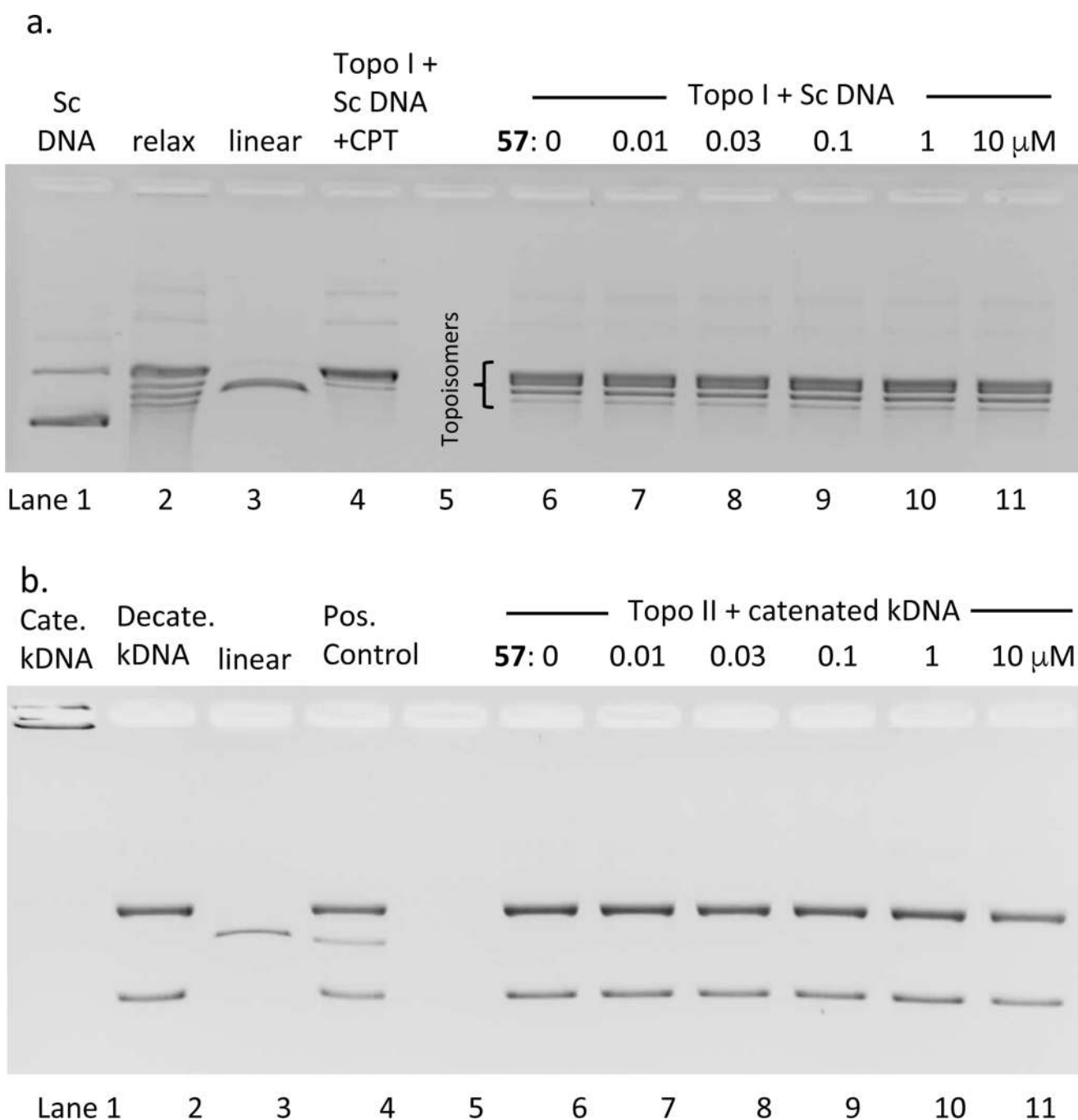


Figure 1. Dose-response curves of enantiomeric forms of kibelone C (**3**) and methyl kibelone C (**57**) against HCT116 colon cancer cells. Cell viability was determined with CellTiter-Glo®.



Figures 2.

a. Interaction of (–)-methyl kibdelone C (**57**) with topoisomerase I (Topo I). Supercoiled plasmid DNA (Sc DNA, lane 1) is converted to relaxed plasmid DNA (lane 2) by Topo I. Linear DNA is shown for comparison (lane 3). Topo I generates nicked open circular DNA, which runs as a single band (lane 4). Methyl kibdelone does not inhibit Topo I up to 10 μ M (lanes 6–11). b. Interaction of **57** with topoisomerase II. Catenated kinetoplast DNA (Cate. kDNA, lane 1) is converted to decatenated kDNA (lane 2) by topoisomerase II. A positive

control, etoposide, induced the formation of linear DNA (lanes 3, 4). Methyl kidelone does not inhibit Topo II up to 10 μ M (lanes 6–11).

Author Manuscript

Author Manuscript

Author Manuscript

Author Manuscript

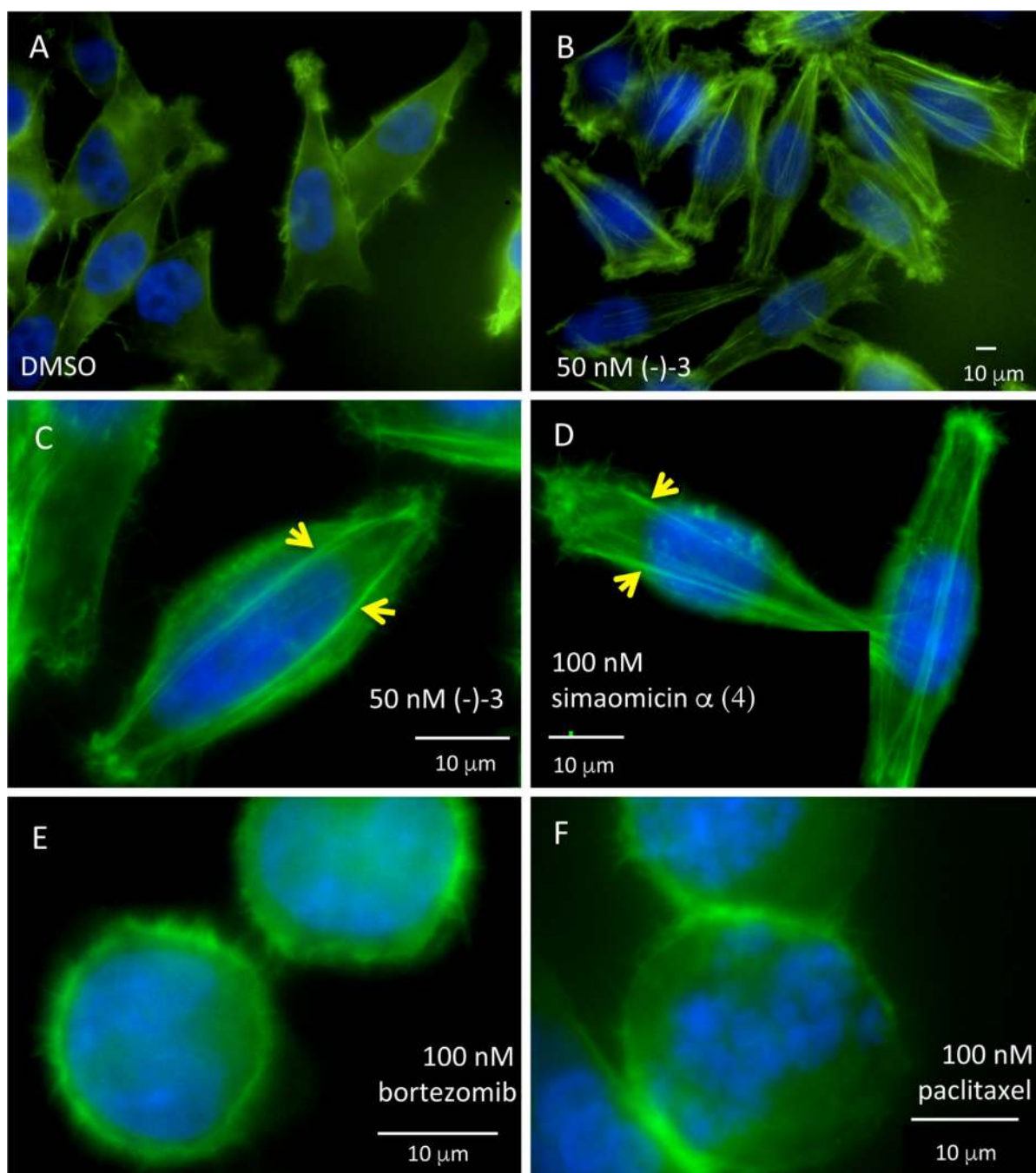


Figure 3. HeLa cells treated with A) DMSO, B) and C) kibdelone C [(-)-**3**], D) simaomicin α (**4**), E) bortezomib or F) paclitaxel for 12h. Representative stress fibers indicated with yellow arrow. Staining of nuclei (blue, DAPI) and actin (green, FITC-phalloidin) reveals cell contraction and stress fiber formation in the kibdelone and simaomicin α -treated cells.

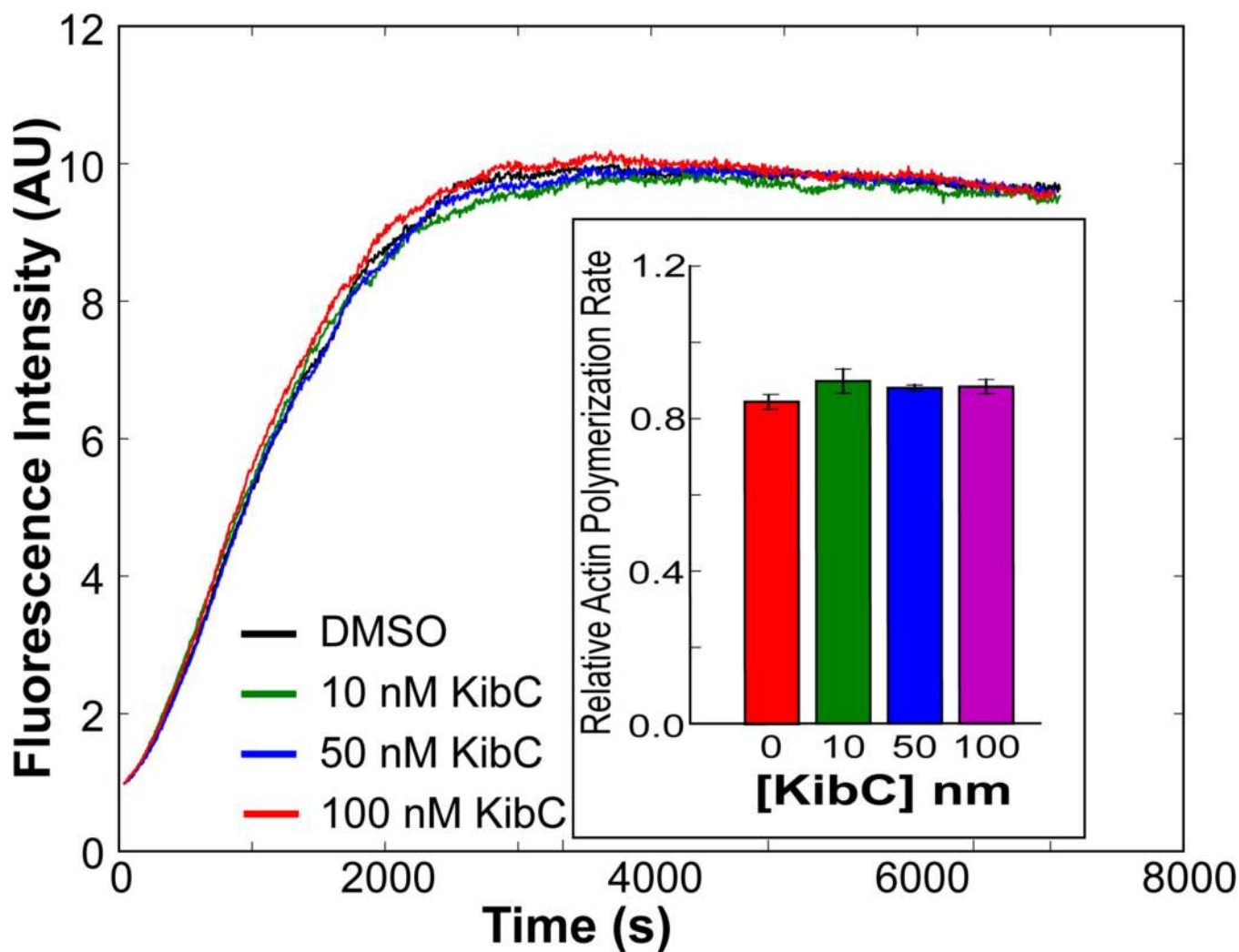
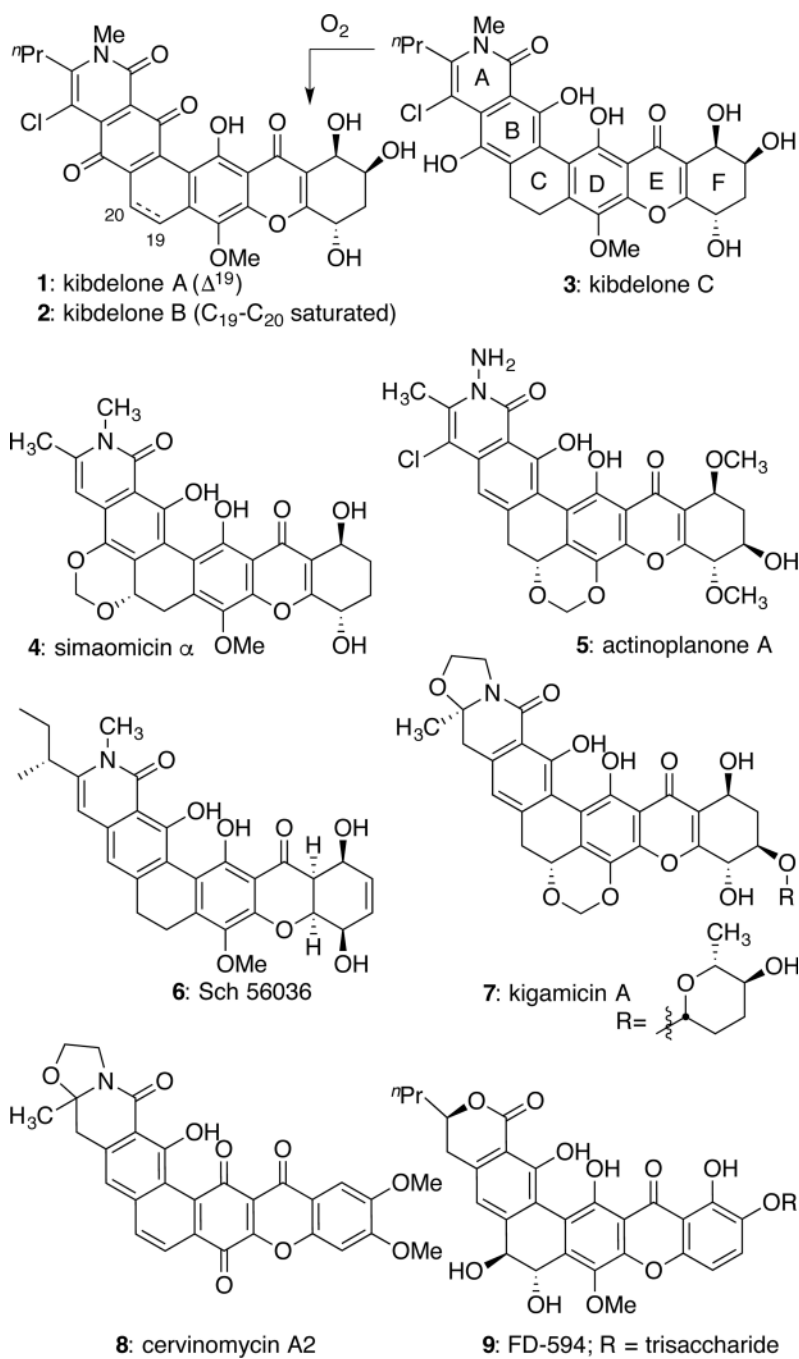
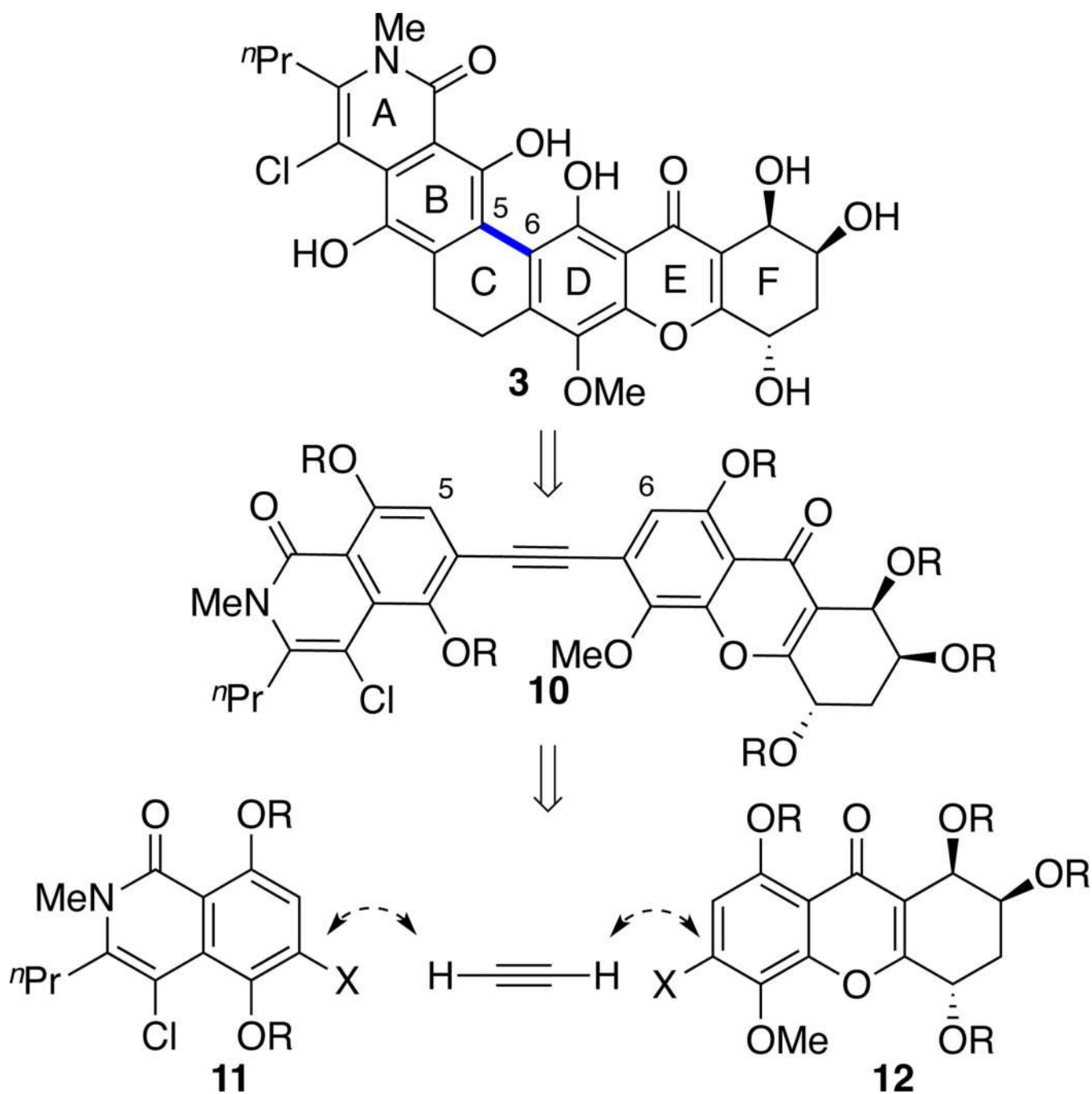


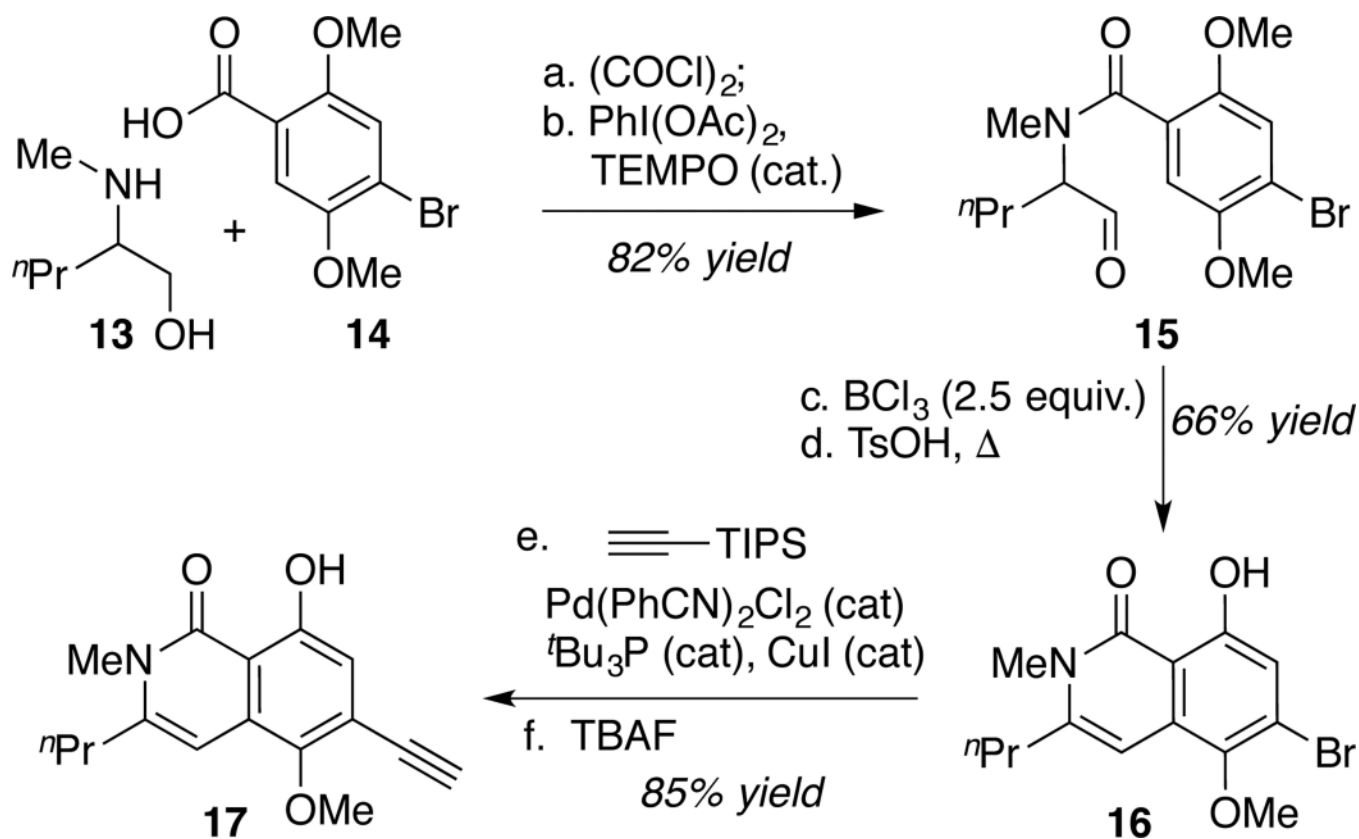
Figure 4. (–)-Kibdelone C (**3**) has no effect on the polymerization rate of actin. The main chart shows the changes in fluorescence as recombinant actin was polymerized over time (2 μ M actin including 10%-pyrene labeled protein). Single experiments are shown in the absence or presence of the indicated concentrations of **3**. Inset shows the average rate of polymerization in the absence or presence of **3** relative to the rate in the absence of DMSO ($n = 3$).



Scheme 1.
Hexacyclic tetrahydroxanthone and xanthone natural products.

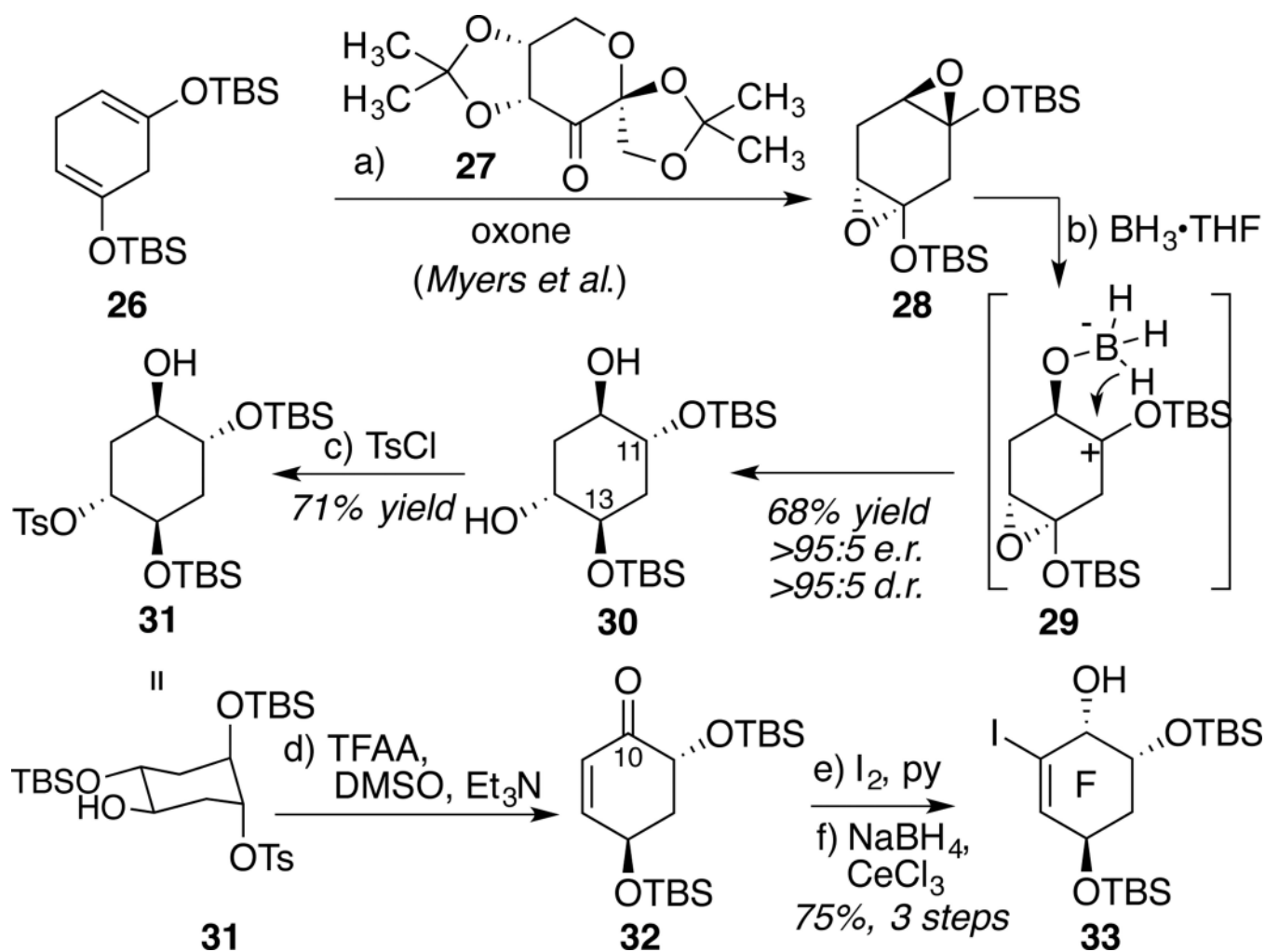


Scheme 2.
Synthetic strategy

**Scheme 3.**

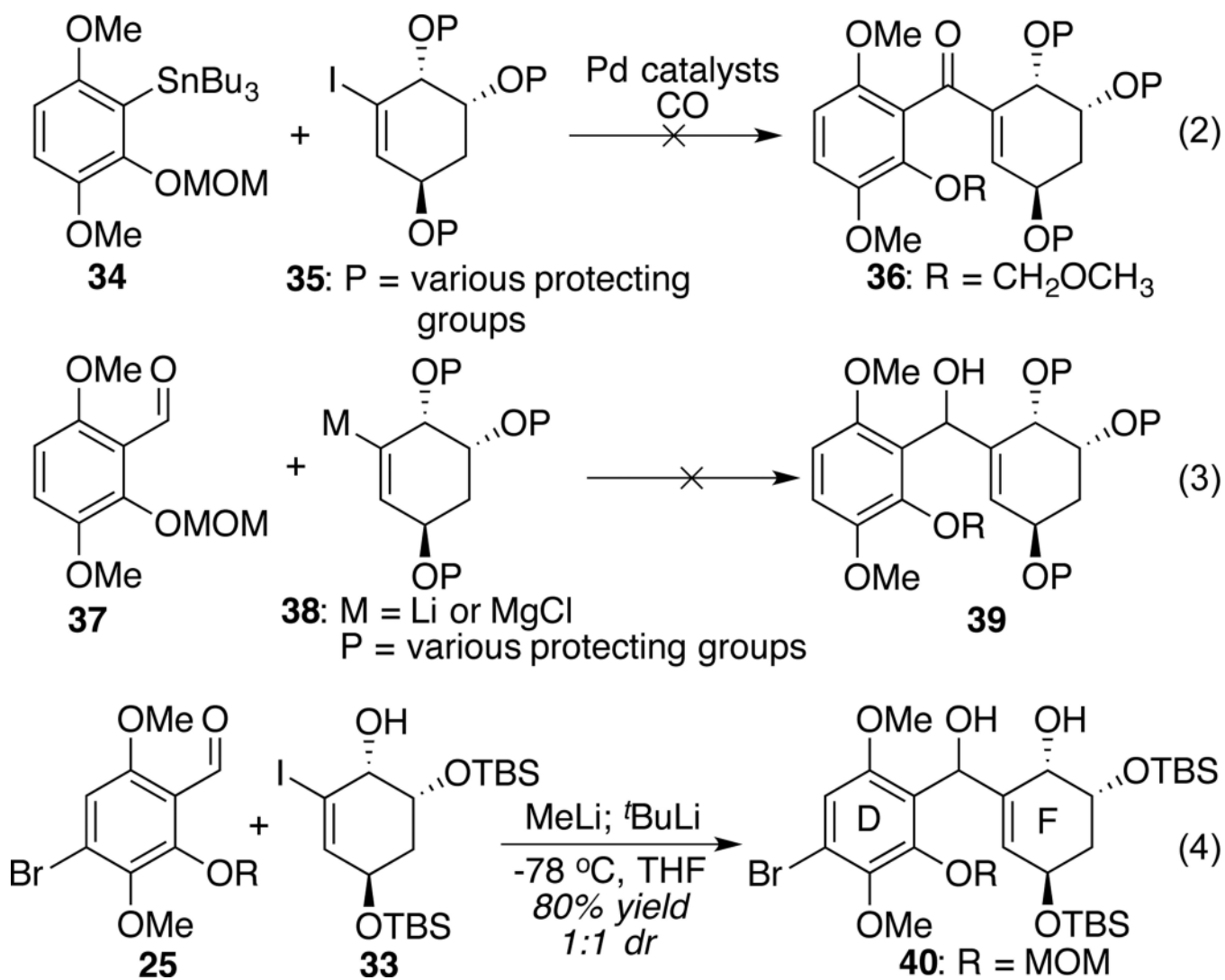
Synthesis of the AB-ring isoquinolinone.

(a) $(\text{COCl})_2$, DMF (cat), CH_2Cl_2 ; $\text{CH}_2\text{Cl}_2/5\text{M NaOH}$ 1.5:1. (b) $\text{PhI}(\text{OAc})_2$, TEMPO (10 mol %), CH_2Cl_2 , 82% yield over 2 steps. (c) BCl_3 (1.0 equiv, then 1.5 equiv), 0 °C to rt. (d) $\text{TsOH}\cdot\text{H}_2\text{O}$ (1.5 equiv), toluene, reflux, 66% yield over 2 steps. (e) $\text{Pd}(\text{PhCN})_2\text{Cl}_2$ (5 mol %), $t\text{Bu}_3\text{P}\cdot\text{HBF}_4$ (10 mol%), CuI (3 mol%), Et_2NH , 40 °C. (f) Bu_4NF (1.5 equiv), 85% yield over 2 steps.

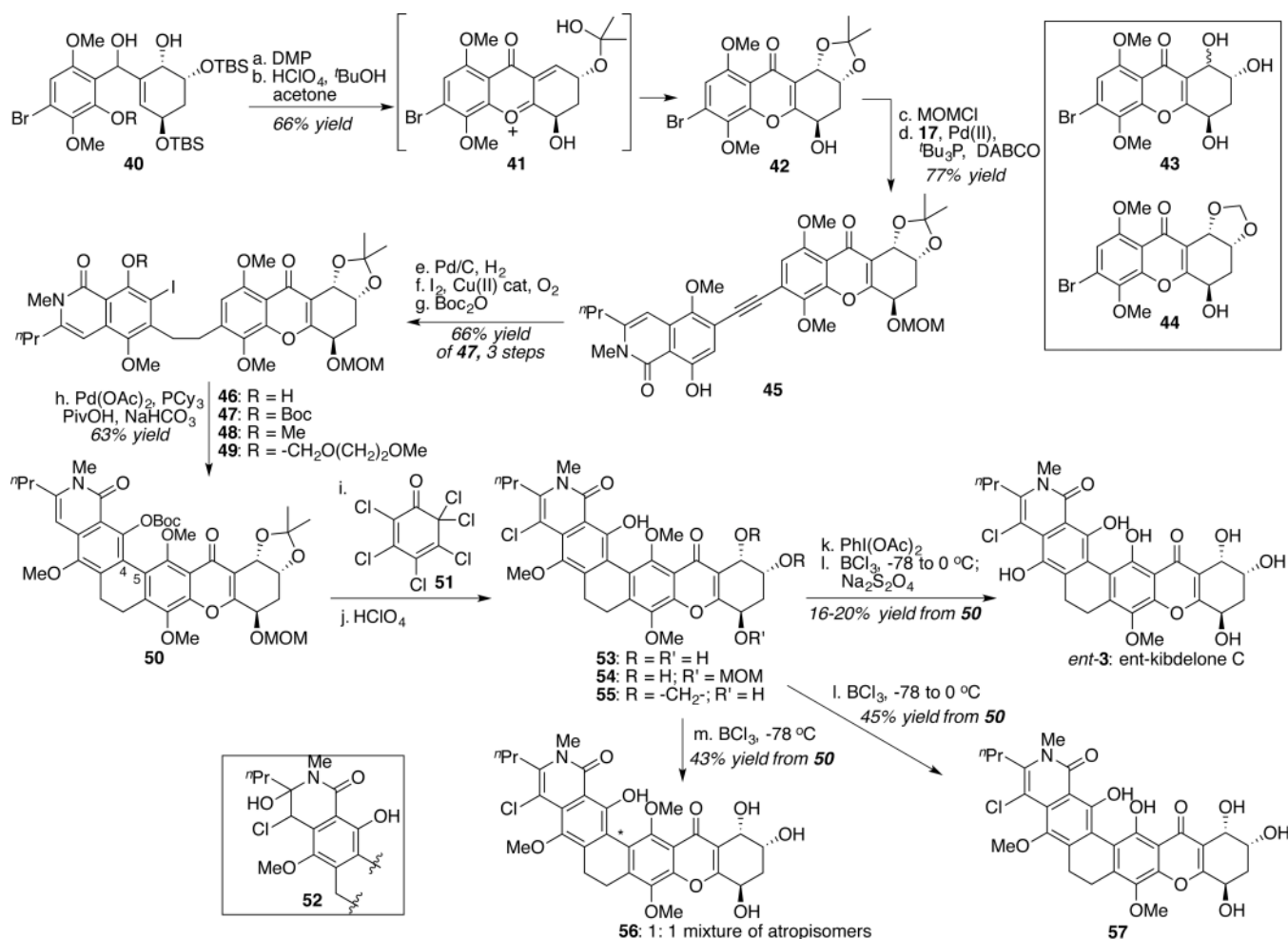
**Scheme 4.**

Enantioselective synthesis of the F-ring

a) Shi catalyst (**27**, 0.6 equiv), oxone, H_2O (pH 10.5), CH_3CN , 0°C , then b) $\text{BH}_3 \cdot \text{THF}$, Et_2O , 0°C , 68% yield over 2 steps, >95:5 e.r. and d.r. c) TsCl, pyridine/ CH_2Cl_2 (1/1). d) TFAA, DMSO, CH_2Cl_2 , then Et_3N , -78°C to rt. e) I_2 , pyridine (1.2 equiv), CH_2Cl_2 . f) NaBH_4 , $\text{CeCl}_3 \cdot 7\text{H}_2\text{O}$, MeOH, -78°C , 75% over 3 steps.

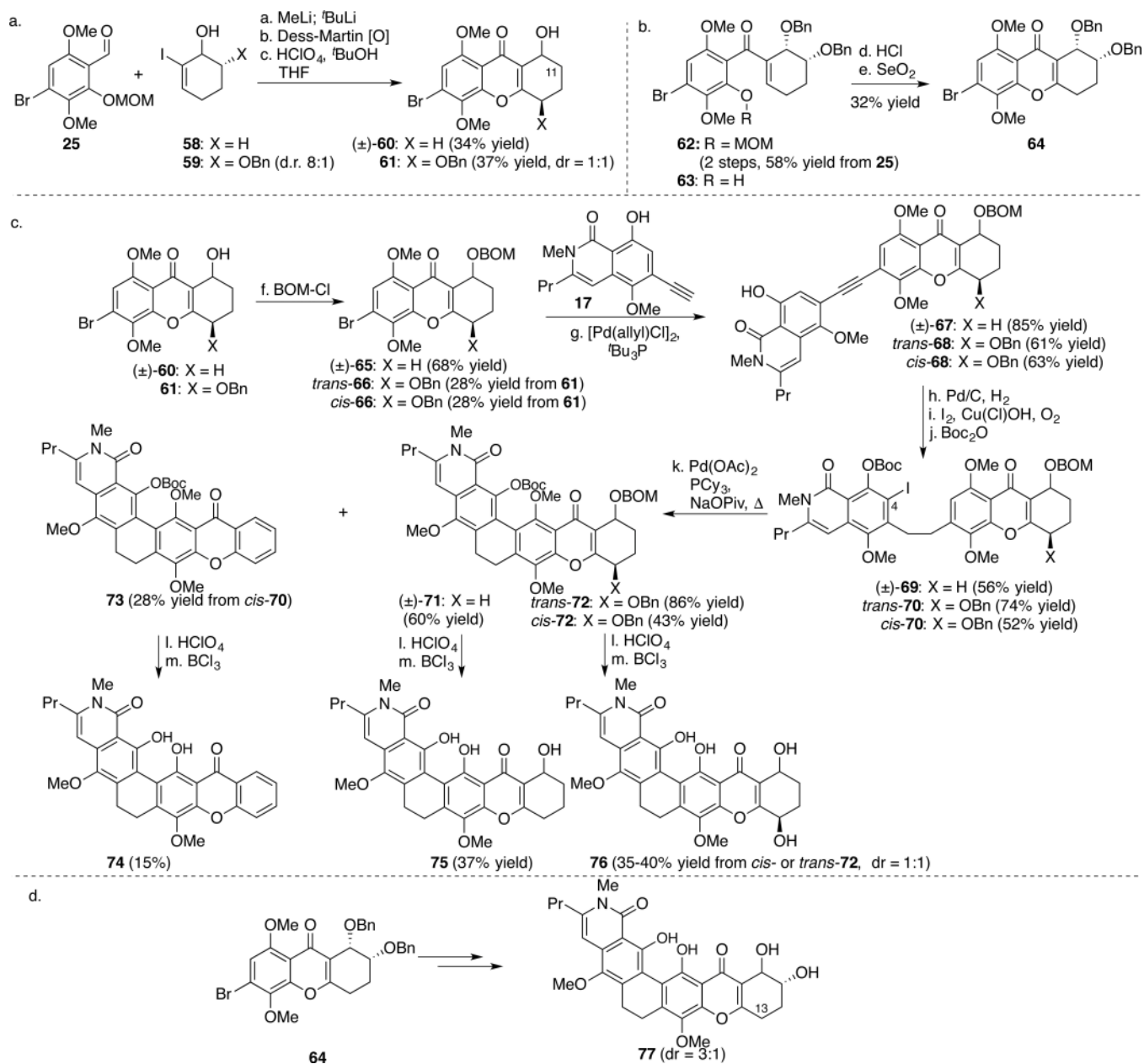


Scheme 5.
Union of the D and F rings.

**Scheme 6.**

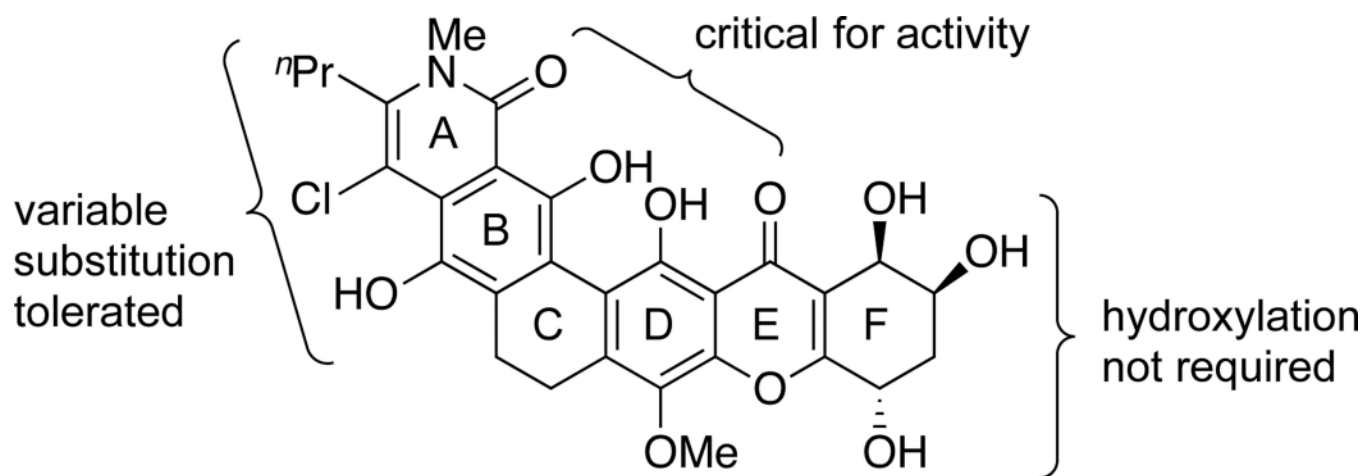
Synthesis of ent-kibdelone C and derivatives

- a) Dess-Martin periodinane, CH_2Cl_2 . b) $\text{HClO}_4(\text{aq})$, $^t\text{BuOH}$, acetone, 66% yield over 2 steps.
 c) MOMCl, $^t\text{Pr}_2\text{NEt}$, CH_2Cl_2 . d) **17**, $[\text{Pd}(\text{C}_3\text{H}_5)\text{Cl}]_2$ (5 mol%), $^t\text{Bu}_3\text{P}$, DABCO, $\text{CH}_3\text{CN}/\text{DMF}$ 1:1, 77% yield, 2 steps. e) 10% Pd/C, NaHCO_3 (1.5 equiv), $\text{CH}_2\text{Cl}_2/^t\text{PrOH}$ (1:1), H_2 . f. CuCl(OH)TMEDA (25 mol%), I_2 , CH_2Cl_2 . g) Boc_2O , DMAP, CH_2Cl_2 . 66% yield over 3 steps. h. Pd(OAc)_2 (1.5 equiv), $^t\text{Bu}_3\text{P}\cdot\text{HBF}_4$ (3.0 equiv), pivalic acid (6.0 equiv), NaHCO_3 (20 equiv), DMA, $90 \text{ } ^\circ\text{C}$, 63% yield, 1:1 mixture of atropisomers. i. **51**, DMF/ CH_2Cl_2 5:1. j. THF/ $^t\text{BuOH}$ 2.5:1, HClO_4 (10 equiv). k. PhI(OAc)_2 (2 equiv), $\text{CH}_3\text{CN}/\text{H}_2\text{O}$ 1:1. l. BCl_3 (6 equiv), CH_2Cl_2 , $-78 \text{ } ^\circ\text{C}$ to $0 \text{ } ^\circ\text{C}$, then $\text{Na}_2\text{S}_2\text{O}_4$. m. BCl_3 (6 equiv), CH_2Cl_2 , $-78 \text{ } ^\circ\text{C}$.

**Scheme 7.**

Synthesis of simplified kibelone C derivatives

- a) **58** or **59**, MeLi (1.05 equiv), Et₂O, then ^tBuLi (2.0 equiv), then **25**, THF, -78 °C. c) HClO₄(aq), ^tBuOH, acetone. d) HCl, THF/H₂O, rt. e) SeO₂ (2.0 equiv), ^tBuOH, reflux. f) Benzyloxymethyl chloride (1.5 equiv), proton sponge (5.0 equiv), NaI (4 equiv), THF, rt. g) [Pd(allyl)Cl]₂ (5 mol%), ^tBu₃P•HBF₄ (20 mol %), DABCO (2.2 equiv), slow addition of **17**, 50 °C. h) Pd/C, H₂ (1 atm), CH₂Cl₂/ⁱPrOH 1:1, rt. i) Cu(Cl)OH•TMEDA (0.25 equiv), I₂ (1 equiv), O₂ (1 atm), CH₂Cl₂, rt. j) (Boc)₂O, DMAP, CH₂Cl₂, rt. k) Pd(OAc)₂ (1.5 equiv), ^tBu₃P•HBF₄ (3.0 equiv), pivalic acid (6.0 equiv), NaHCO₃ (20 equiv), DMA, 90 °C. l) THF/^tBuOH 2.5:1, HClO₄ (10 equiv), m) BCl₃ (6 equiv), CH₂Cl₂, -78 °C to 0 °C.



Scheme 8.
Structure-activity relationship

Table 1

Formylation and hydroxymethylation of the D-ring.

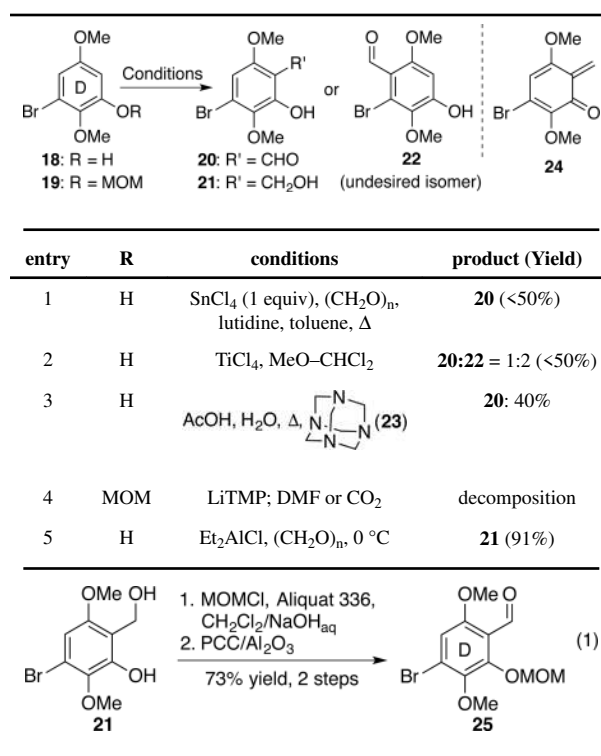
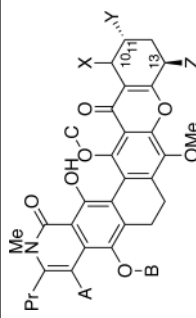


Table 2

Cytotoxicity of synthetic derivatives of kibelone C vs. non-small cell lung cancer cell lines.^a



Compound	Cell line/ IC ₅₀ (nM)						
	A	B	C	X	Y	Z	H2122
3 :(-)-kibelone C	Cl	H	H	β-OH	OH	OH	23
3 :(+)-kibelone C	Cl	H	H	β-OH	OH	OH	40
56	Cl	CH ₃	CH ₃	β-OH	OH	OH	4760
57	Cl	CH ₃	H	β-OH	OH	OH	11
74	H	CH ₃	H	— aryl F ring	—	—	22
75	H	CH ₃	H	OH	H	H	38
76	H	CH ₃	H	OH	H	OH	1
77	H	CH ₃	H	OH	OH	H	3

^aCell viability measured with CellTiter-Glo®. IC₅₀ values calculated from 12 point dose-response curve in triplicate.

Table 3Impact of exogenous DNA on cytotoxicity of natural products.^a

compound	IC ₅₀ (nM) in presence of added DNA ^b			
	0 μ g	4 μ g	12 μ g	40 μ g
actinomycin	0.5	1.5	5.9	51
paclitaxel	6.4	7.8	7.2	6.4
kibdelone C	67	43	64	61

^aHerring sperm DNA was added to H2122 cell cultures at the indicated levels in 96-well plates, and cells were incubated for 4 days prior to quantifying cell viability with CellTiter-Glo[®].

^bCalculated concentrations at which there were 50% fewer viable cells compared to DMSO control.